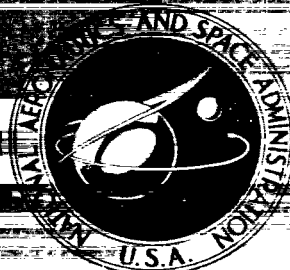


**NASA CONTRACTOR
REPORT**



NASA CR-15

0060848

TECH LIBRARY KAFB, NM

NASA CR-1538

LOAN COPY: RETURN TO
AFWL (WL01)
KIRTLAND AFB, N MEX

OBSERVATION OF FLOW EXCURSIONS IN A SIMULATED GAS-COOLED REACTOR PASSAGE

by Paul Vingerhoet, Edward R. Kolbe, and Eli Reshotko

Prepared by
CASE WESTERN RESERVE UNIVERSITY
Cleveland, Ohio
for Lewis Research Center



NATIONAL AERONAUTICS AND SPACE ADMINISTRATION • WASHINGTON, D. C. • FEBRUARY 1970



0060848

1. Report No. ✓ NASA CR-1538	2. Government Accession No.	3. Recipient's Catalog No.	
4. Title and Subtitle ✓ OBSERVATION OF FLOW EXCURSIONS IN A SIMULATED GAS-COOLED REACTOR PASSAGE		5. Report Date February 1970 ✓	
		6. Performing Organization Code	
7. Author(s) <i>omit</i> Paul Vingerhoet, Edward R. Kolbe and Eli Reshotko		8. Performing Organization Report No. None	
9. Performing Organization Name and Address <i>corp. au 1</i> Case Western Reserve University Cleveland, Ohio 44106		10. Work Unit No.	
		11. Contract or Grant No. NGR 36-003-064 <i>omit</i>	
12. Sponsoring Agency Name and Address National Aeronautics and Space Administration Washington, D.C. 20546		13. Type of Report and Period Covered Contractor Report	
		14. Sponsoring Agency Code	
15. Supplementary Notes			
16. Abstract The steady state characteristics of helium gas flowing in an electrically heated Nichrome V tube 0.094" ID by 54" long were obtained for laminar, transitional and turbulent flow. Excursions at constant pressure drop from an unstable laminar equilibrium point to a stable turbulent equilibrium point were triggered and observed. The results substantiated the theory of Reshotko in showing that the time-history of an excursion is directly related to the heat capacity of the core and that an excursion is non-violent and non-oscillatory in nature.			
17. Key Words (Suggested by Author(s)) Laminar flow Turbulent flow Heat transfer Gas-cooled reactor passage		18. Distribution Statement Unclassified - unlimited	
19. Security Classif. (of this report) ✓ Unclassified	20. Security Classif. (of this page) Unclassified	21. No. of Pages 33	22. Price* \$3.00

*For sale by the Clearinghouse for Federal Scientific and Technical Information
Springfield, Virginia 22151

Distribution of this report is provided in the interest of information exchange. Responsibility for the contents resides in the author or organization that prepared it.

FOREWORD

The research described herein was conducted at the School of Engineering, Case Western Reserve University, under NASA Grant NGR 36-003-064 with John C. Evvard, NASA Lewis Research Center, as Technical Manager.

OBSERVATION OF FLOW EXCURSIONS
IN A SIMULATED GAS-COOLED REACTOR PASSAGE

By Paul Vingerhoet^{*}, Edward R. Kolbe^{**} and Eli Reshotko
Case Western Reserve University
Cleveland, Ohio

SUMMARY

In the present work the steady state characteristics of helium gas flowing in an electrically heated Nichrome V tube 0.094" ID by 54" long were obtained for laminar, transitional and turbulent flow. Excursions at constant pressure drop from an unstable laminar equilibrium point to a stable turbulent equilibrium point were triggered and observed. The results substantiated the theory of Reshotko in showing that the time-history of an excursion is directly related to the heat capacity of the core and that an excursion is non-violent and non-oscillatory in nature.

* Graduate Student, now at Raytheon Company, Bedford, Mass.

** Graduate Student, now at Hamilton Standard Div., United Aircraft Corp.

INTRODUCTION

When the thrusting "burn" of a nuclear rocket engine is terminated, some subsequent coolant flow is still required to remove the afterheat due to fission product decay. The amount of cooling required may be sufficiently low for laminar flow to exist in the core passages.

In the relevant analysis of the steady flow of a gas in a tube with friction and heat addition, one finds some interesting peculiarities. At a constant heat rate to the gas the pressure drop versus flow rate curves are concave upward in the laminar-turbulent flow regime. This general shape indicates the existence of two possible flow rates for any given pressure drop at a constant heat rate to the gas. The outlet-to-inlet gas temperature ratio decreases monotonically with increasing flow rate in the laminar-turbulent transition region. A representative set of steady-state characteristics are sketched in Fig. 1, where for any given flow rate the pressure drop increases with \bar{Q} as shown. The temperature ratio corresponding to the minimum pressure drop for any constant heat rate curve is termed the "critical" temperature ratio. For temperature ratios greater than critical the change of pressure drop with flow rate at constant heat rate to the gas is negative. This negative slope is associated with laminar flow. For temperature ratios less than critical the slope is positive and the flow is usually turbulent.

Much attention has been devoted to the left or laminar portion of the steady-state characteristic curves since this portion of the curve is believed to be unstable; in fact the instability has been termed a "laminar instability". As a result of this laminar instability spontaneous flow excursions to higher or lower flow rates are presumed to take place if one were to operate on the negatively sloped portion of a steady-state characteristic curve, assuming

that the pressure drop is held constant.

These characteristics have been noted theoretically¹⁻⁵ and have also to some extent been observed in the laboratory⁶⁻¹⁰. The purpose of the present study is threefold: first, to design and construct an apparatus for the investigation of the "laminar instability" problem; second, to obtain as extensive a set as possible of steady-state operating data for a single flow passage; and third, to experimentally trigger and observe an excursion at constant pressure drop from an unstable laminar equilibrium point on the negatively sloped portion of a steady-state characteristic curve to the corresponding stable turbulent equilibrium point on the positively sloped portion of the same steady-state characteristic curve. The experimental results will in each case be compared with theoretical predictions. Excursions to lower flow rates will not be discussed herein.

SYMBOLS

A	Cross-sectional flow area
a	Cross-sectional area of "reactor core" associated with single passage
c	Specific heat of "core" material
C_p	Specific heat at constant pressure of coolant
d	Tube internal diameter
f	Fanning friction factor
g	Gravitational acceleration
h	Forced convection heat transfer coefficient
I	Current
L	Tube length
m	Density of "reactor core" material
m	Exponent of viscosity variation with temperature, $\mu = \mu_0 T^m$
n	Exponent of friction factor variation with Reynolds number, $f = f_0 / Re^n$
p	Pressure
Δp	$P_1 - P_2$
Q	Heat rate per unit inside surface area of tube
\bar{Q}	Average heat rate to gas per unit inside surface area of tube
R	Gas constant
r_h	Hydraulic radius ($r_h = d/4$ for round tubes)
T	Absolute temperature
τ	Dimensionless time unit
t	Time

V	Voltage
W	Mass flow rate
μ	Viscosity
ϕ	Reactor energy release rate
τ	Final-to-initial gas temperature ratio

Subscripts

o	Initial constant
0	Value at unstable equilibrium point
1	Conditions at entrance to the flow passage
2	Conditions at exit of the flow passage
w	Conditions at wall
b	Evaluated at bulk conditions
f	Evaluated at film conditions
avg	Average
max	Maximum

APPARATUS DESIGN

A major objective of the present work was to design and construct an apparatus which would enable study of both the static and dynamic phenomena occurring in parallel reactor passages⁹. A tube bank consisting of one, two, and possibly three heated flow passages was planned. It was felt that these passages when connected to common headers would closely simulate a

reactor situation. However, by using only one tube in the apparatus at first, it was felt that flow excursion phenomena could be adequately investigated.

Before actual apparatus design could begin, various preliminary calculations of flow characteristics accompanying different gases, tube geometries, and heating rates were performed. Use was made of the non-dimensional parameters formulated by Harry ³ to obtain rough results. Although hydrogen gas is the fluid of primary consideration in the actual nuclear rocket case, it was rejected for safety reasons. Helium gas was found to exhibit much the same flow behavior under safer, more easily maintained and measured conditions. Helium is a desirable gas to use because it is inert and many of its properties e.g., conductivity, specific heat, and viscosity are relatively close to those of hydrogen.

An inlet temperature of 140°R was selected as the lowest temperature which could be easily obtained; it is the temperature of boiling liquid nitrogen.

The initial design and construction was done with a view toward experimentation with only one test passage. However, flow rate predictions and plenum design were done in such a way that two parallel tubes could be used in future operation.

A closed loop system was used (see Fig. 2) since it was economically desirable to conserve the helium.

The test section was made from Nichrome V (80% nickel, 20% chromium) tubing. Its dimensions .094" inside diameter, 4.5' length, and .020" wall thickness supported desirable flow characteristics. The advantage of Nichrome was its small variation of resistivity with temperature, making electrical resistance heating a good method of simulating a "heated reactor passage". *

* Data ¹¹ indicates that the resistivity of heavy Nichrome wire will increase no more than a few percent during heating from room temperature to 2000°F. While this variation would lead to some non-uniformity in heat rate, it would not affect the nature of the experiment.

In an effort to minimize heat losses which in general would increase with an increase in wall temperature, the test section was placed in a vacuum chamber whose pressure was sufficiently low to eliminate significant convection heat transfer from the outside of the tube. Thermal expansion of the tube required use of a spring suspension system which would maintain a tension on the tube at all times. This and the presence of a liquid nitrogen heat exchanger necessitated the placing of the entire assembly, i.e., heat exchanger, test section, and inlet and outlet plenums, inside the vacuum tank. The tank and assembly are shown in Fig. 3.

As seen in Fig. 2 pressures in the inlet and outlet plenums were controlled by regulators whose inlet flow was supplied from a high pressure reservoir. Another low pressure or vacuum reservoir in the line upstream of the circulating pump provided a low pressure dump for the flow leaving the test section and outlet plenum regulator.

Gas temperatures in the inlet and outlet plenums were measured by copper-constantan and shielded chromel-alumel thermocouples respectively. Five thermocouples silver-soldered to the test section enabled wall temperature distributions to be measured. Maximum wall temperatures encountered in the tests were well below the melting point of silver solder. Pressure drop across the test section was read from a transducer indicator; all other pressures of interest were measured with gauges. During initial testing, it would be possible to operate with an inlet pressure, p_1 , between 0 and 20 psig, a pressure drop, Δp , of up to 10 psi, and an electrical power capacity corresponding to a heat rate of up to 96.4 watts.

STEADY STATE OPERATION

One-Dimensional Flow Analysis

An approximate solution to the steady one-dimensional flow of a perfect gas in a constant-area flow passage with friction and heat addition was obtained by Harry³. Harry's result for the case of uniform heat addition is

$$P_{avg} \Delta p = \frac{RT_1}{g} \left(\frac{W}{A} \right)^2 \left[(\tau - 1) + \frac{f_o \mu_1^n L}{2r_h \left[4r_h \left(\frac{W}{A} \right) \right]^n} \frac{1}{(mn + 2)} \frac{\tau^{mn+2} - 1}{(\tau - 1)} \right] \quad (1)$$

The first term in the square brackets represents the momentum pressure drop while the second term represents the frictional pressure drop. At low flow rates the frictional pressure drop dominates and at high flow rates the momentum pressure dominates.

Steady-State Flow Characteristics

In the present investigation helium gas enters the flow passage at liquid nitrogen temperature (140°R). The steady-state characteristics were calculated using Eq. (1). For laminar flow $f_o = 16$, $n = 1$, $m = 0.65$, and for turbulent flow $f_o = 0.046$, $n = 0.2$, $m = 0.65$. The results of these calculations are shown in Fig. 4 for a number of gas heating rates.*

Remember that in the steady-state all the heat, Q , goes into heating the gas. The energy equation for the gas can be written simply as,

$$\left(\frac{W}{A} \right) C_p (T_2 - T_1) = Q \left(\frac{L}{r_h} \right)$$

or in terms of the temperature ratio, τ

$$\left(\frac{W}{A} \right) C_p (\tau - 1) = Q \left(\frac{L}{r_h T_1} \right)$$

* The properties of helium used herein are those of Reference 12.

Fig. 4 shows that the pressure drop versus flow rate curves for constant heat rate to the gas are concave upward. This indicates the existence of two flow rates for any constant pressure drop. The temperature ratio is inversely proportional to the flow rate for a constant heat input to the gas.

According to Harry³ the flow is arbitrarily chosen as laminar up to a Reynolds number of 2100 and turbulent down to a Reynolds number of 1000, where the Reynolds number is evaluated at the film temperature, $[T_f = (T_w + T_b)/2]$. In this investigation the same criterion was employed except that the Reynolds number was evaluated at the bulk gas temperature. Turney, Smith, and Juhasz substantiate, by experiment, that this procedure yields reasonable results.

Test Procedure

Before any data were taken both the helium loop and vacuum chamber surrounding the test section were purged to the atmosphere. They were then evacuated to a vacuum of approximately 0.01 torr. The vacuum chamber was sealed off from the helium loop by closing the shut-off valve connecting the two. The helium loop was filled with helium gas from a high pressure storage tank to a pressure of 18 psig. The liquid nitrogen was then allowed to flow through the heat exchanger. The helium circulating pump and electrical heating were turned on. The inlet pressure was adjusted to 1 psig. The pressure drop (independent variable) was controlled by the pressure regulator downstream of the test section while the flow rate (dependent variable) was read from a rotameter.

The system was assumed to be in steady-state when all the indicators were reading constant values.

The steady-state characteristics relating pressure drop and temperature ratio with flow rate for various electrical heat rates are shown in Fig. 5. These data were obtained for a given electrical heat rate by increasing the pressure drop, using the downstream pressure regulator, from approximately .25 to 4.0 psi. The pressure drop was increased in increments. After each

increase it took several minutes to reach steady-state conditions. When steady-state conditions prevailed the appropriate measurements were taken. The constant electrical heating curves in Fig. 5 were reproducible to within approximately 7%.

In calculating the average heat rate to the gas, \bar{Q} , using the equation $\bar{Q} = \left(\frac{W}{A} \right) C_p (T_2 - T_1)$ it was found that \bar{Q} varied significantly along curves of constant electrical heat input as seen by Fig. 6. Ideally (in the steady-state solution) all electrical heating should go into heating the gas. Therefore, it was concluded that there were considerable heat leaks to the test section. The heat leaks were such that even at zero electrical heating there was substantial heating of the gas. An analysis of the heat losses was attempted, but not all of the heat losses could be accounted for satisfactorily.

Nevertheless it was still possible to generate the steady-state characteristics for constant \bar{Q} by connecting points of equal \bar{Q} on each of the curves of constant electrical heating. These curves are shown in Fig. 7. In the same manner the temperature ratios for constant \bar{Q} are also plotted in Fig. 7. Using the technique just described it was possible to generate the steady-state operating characteristics in the form illustrated in Fig. 1.

In comparing the theoretically calculated steady-state results of Fig. 4 with the experimental results of Fig. 7, the degree of agreement depends significantly on whether the flow is laminar or turbulent. In the turbulent region the pressure drop is in agreement to within approximately 10%. In the laminar region, however, the experimentally observed pressure drop tends to be as much as 56% greater than predicted using Eq. (1). The agreement is better for higher flow rates and poorer for lower flow rates.

One might explain this rather poor agreement with theory in the following manner. In the laminar region the frictional pressure drop dominates in the equation for pressure drop. Since the frictional pressure drop is a strong function of viscosity, thus temperature, it is thought that better agreement

would have been established if the viscosity had been evaluated at the film temperature. Better agreement might have followed if the friction factor had accounted for radial temperature variations. Turney, Smith and Juhasz⁸ accounted for both of these effects and also the pressure losses due to entrance and exit geometry. By numerically computing the pressure losses in successive segments of their test section they achieved theoretical results which agreed with experiment to within 10%. Their apparatus was of similar construction to that of the present investigation except that they used normal hydrogen gas as the test fluid and measured the wall temperature every few inches.

In the turbulent flow region the dominant pressure drop is that of the momentum change and the effects mentioned above have a negligible contribution to the pressure loss.

Remember also that the electrical heating is not strictly uniform and that Eq. (1) is only an approximate solution for estimating the pressure drop with uniform heat addition.

It might also be mentioned here that in trying to operate the apparatus at low pressure drops, spontaneous oscillations in pressure drop, flow rate, and temperatures were sometimes observed. It is thought that these oscillations were in no way related to the instabilities or flow excursions of the kind discussed herein. Rather, they are thought to be a result of some mechanical instability related to the construction of the apparatus (there were considerable vibrations in parts of the helium loop caused by the vibrations of the circulating pump). By manually increasing the pressure drop to a point where the oscillations ceased and after several attempts at slowly decreasing the pressure drop, the low pressure drop operating points could be satisfactorily obtained in steady operation.

Stability of One-Dimensional Flow With Constant Pressure Drop

A time-dependent stability analysis was performed in Ref. 5 using a perturbation technique. Results affirm the commonly accepted criterion that flows of the type discussed herein are subject to instabilities when the change in pressure drop with weight flow at constant heat rate to the gas is negative, i.e., instabilities may occur when

$$\frac{\partial(\Delta p)}{\partial \left(\frac{W}{A} \right)_{\bar{Q}}} < 0$$

One physically explains the instability and flow excursions at constant pressure drop as follows: if a flow passage were being operated at an equilibrium point on the left leg of the U-shaped characteristic curves shown in Fig. 7, an excursion at constant pressure drop to a higher flow rate would require additional heat to the gas. This heat would be provided by further cooling of the core and the excursion would continue; in an excursion from the same equilibrium point to a lower flow rate at constant pressure drop the gas requires less heat. Thus the additional heat goes into heating the core. Therefore, one concludes that the left or laminar leg is unstable since unbounded excursions at constant pressure drop may occur. For completeness excursions at constant pressure drop are now examined for the right leg. Operating on an equilibrium point on the right leg an excursion to higher flow rate at constant pressure drop would require a decrease in the heat rate to the gas and since the core is being cooled by this increase in flow rate there is an increase in the heat rate to the gas and the flow is driven back to the equilibrium point. An excursion at constant pressure drop to lower flow rate requires an increase in the heat rate to the gas and to the core, but since the heat generation rate of the reactor is constant the flow reverts back to the equilibrium point. Therefore, the higher

- flow rate equilibrium point is stable.

Excursions at Constant Pressure Drop

The analysis of an excursion at constant pressure drop was also done in Ref. 5. The time for an excursion is given in dimensionless time units, T , that are related to physical time by

$$T \equiv \frac{1}{m} \frac{A}{a x_h} \left(\frac{h_1}{c} \right)_0 t \quad (2)$$

While the steady-state flow and heat transfer characteristics of a flow passage are dependent solely on the fluid and internal geometry of the flow passage, the time for an excursion is related to the heat capacity of the core as shown in Eq. (2).

The time in dimensionless time units for an excursion to higher flow rate at constant pressure is given by

$$T = \int_{\tau_1}^{\tau} \frac{\frac{d\bar{Q}}{d\tau} \left\{ 1 + XY - (1-n) \frac{d \ln \left(\frac{W}{A} \right)}{d \ln \bar{Q}} \right\}_{\Delta p}}{\frac{h_1}{(h_1)_0} \left[\frac{\tau^{mn+1} - 1}{(\tau - 1)(mn + 1)} \right] [\bar{Q}_0 - \bar{Q}]} d\tau \quad (3)$$

where X and Y are defined as

$$X \equiv \left[\frac{h_1 T_1}{Q} \left\{ \frac{(mn + 2)(\tau - 1)\tau^{mn+1} - (\tau^{mn+2} - 1)}{(mn + 1)(mn + 2)(\tau - 1)} \right\} - mn \left(1 - \frac{\ln \tau}{\tau - 1} \right) \right]$$

$$Y \equiv \left[1 - \frac{d \ln \left(\frac{W}{A} \right)}{d \ln Q} \right]_{\Delta p}$$

Equation (3) can be evaluated numerically from any set of steady-state operating curves. For example, in this investigation Eq. (3) was solved for the steady-state characteristics of Fig. 7.

Test Procedure

All flow excursions were run at a constant pressure drop of 1 psi. The constant heating curve of $\bar{Q} = 0.376 \text{ BTU/sec-ft}^2$ was chosen as the steady-state heating curve on which to base the excursions. Therefore, as seen in Fig. 8 the excursion would run from $\bar{Q}_0 = 0.376$ (IV = 96.4 watts, $\frac{W}{A} = 1.17 \text{ lbm/sec-ft}^2$) to $\bar{Q} = .376$ (IV = 0 watts, $\frac{W}{A} = 2.90 \text{ lbm/sec-ft}^2$) at a constant pressure drop of 1 psi.

The excursion was initiated by operating on the "unstable" laminar equilibrium point of the left leg of the steady-state operating curve at $\bar{Q}_0 = .376 \text{ BTU/sec-ft}^2$, $\Delta p = 1 \text{ psi}$. The electrical heating was then shut off to trigger the excursion. During the excursion the pressure drop and inlet pressure were manually adjusted to maintain constant values of 1 psi and 1 psig respectively. The gas exit temperature and flow rate measurements were recorded at successive time intervals. The time-history results of such an excursion are shown in Fig. 9. The curves shown are the average of three close runs that are within 5% of each other.

Looking at Fig. 9 one sees that the general shape of an excursion curve (i.e., the time-history of \bar{Q}) is described as follows: there is a gradual increase in \bar{Q} as the excursion first proceeds away from the unstable equilibrium point; a rapid increase; a maximum; a rapid decrease followed by a gradual decrease in \bar{Q} to its final stable equilibrium point corresponding to the original value of \bar{Q} . Since the shape and duration of the initial increase in \bar{Q} is directly dependent on the means and magnitude of the initial perturbation, the most meaningful way of comparing theory with experiment is perhaps to compare the time it takes to go from 1/2 maximum (1/2 rise), approaching \bar{Q}_{\max} , to 1/2 maximum (1/2 fall), leaving \bar{Q}_{\max} .

In the calculation of the excursion characteristics from Eq. (3), one must know the value of \bar{Q}_0 . In analyzing a nuclear reactor flow passage \bar{Q}_0 is equal to the heat rate to the gas at the initial unstable equilibrium point and from

$$\bar{\phi}_0 \mathcal{Q} r_h / A = \bar{Q}_0$$

thus \bar{Q}_0 is constant during an excursion since $\bar{\phi}_0$ is constant. Since it was impossible to keep $\bar{\phi}_0$ (the equivalent of reactor energy release rate) constant during an excursion on the present apparatus an upper and lower limit of the value of \bar{Q}_0 as a function of flow rate had to be established. A lower limit of \bar{Q}_0 was chosen as that value of \bar{Q} which corresponded to the zero electric power input corresponding to the appropriate flow rate (Fig. 5). The upper limit of \bar{Q}_0 was chosen as $0.376 \text{ BTU/sec-ft}^2$ (initial equilibrium value) and was kept constant during the excursion calculations. The actual time for an excursion would be expected to fall somewhere in between these upper and lower limit calculations. A sketch indicating the upper and lower limits of \bar{Q}_0 is shown in Fig. 10.

The characteristic time was found from Eq. (2) to be 19.3 seconds, (i.e., $1T = 19.3 \text{ sec}$). This characteristic time is the same for all the excursions observed since the same initial unstable equilibrium point was used for all excursions.

Applying Eq. (3) to the experimentally observed steady-state characteristics of Fig. 7 yields the results shown in Fig. 11 and 12 for $\bar{Q}_0 = \text{constant}$ (upper limit) and $\bar{Q}_0 \neq \text{constant}$ (lower limit) respectively.

In comparing theory (Fig. 11 and 12) with experiment (Fig. 9) one notices a discrepancy in the values of \bar{Q}_{max} . The theoretical curves are however based on the steady-state data of Fig. 7 which were reproducible only to within approximately 7%. Hence the value of \bar{Q}_{max} of Fig. 9 is within expectations. However, because of this difference in the value of \bar{Q}_{max} the times from 1/2 rise to 1/2 fall were compared at an average value of \bar{Q} , i.e., $\bar{Q} = 0.450 \text{ BTU/sec-ft}^2$. Using this procedure one finds that for $\bar{Q}_0 = \text{constant}$ Eq. (3) predicts an excursion time from 1/2 rise to 1/2 fall (at $\bar{Q} = 0.450$) of $6T$, 30% above the experimental value of $4.7T$. For $\bar{Q}_0 \neq \text{constant}$ theory predicts $3.5T$, 28% below the experimental value.

The experimentally observed excursion time would be expected to lie somewhere between the upper and lower limits presented herein and does. Thus the agreement of theory with experiment is certainly reasonable.

Not only does Eq. (3) predict excursion time reasonably well, but the experiment tends to support the notion that an excursion is non-violent and non-oscillatory in nature. Rather it is a steady procession away from an unstable equilibrium point and the characteristic time is intimately connected with the heat capacity of the core (or tube wall as is the case in the experiment).

CONCLUSIONS

In the present investigation steady-state operating characteristics have been obtained experimentally for laminar, transitional and turbulent flow of a gas flowing in a heated tube. Excursions from an unstable laminar equilibrium point to a stable turbulent equilibrium point at constant pressure drop were triggered and observed. It was shown that the time-history of an excursion is directly related to the heat capacity of the core, and that an excursion is non-violent and non-oscillatory in nature.

During an excursion the gas is heated and the heat rate to the gas reaches a maximum at a flow rate just larger than that for a neutral disturbance. The characteristic times were observed to be of the order of seconds to minutes and the excursion was seen to be a steady procession away from an unstable laminar equilibrium point to a stable turbulent equilibrium point. It also tends to support the notion that with the aid of feedback mechanisms a nuclear rocket might be operated in the "unstable" region, since the characteristic time of an excursion in a nuclear rocket would be larger than those observed herein because the specific heat of a reactor core would be larger than that of the Nichrome V tube used in this experiment. Feedback mechanisms might even lead to better efficiencies in operating in the "unstable" laminar region since very high temperature levels

(limited only by core material limitations) may be obtained coupled with relatively low propellant consumption rates, whereas operating in the turbulent stable region one must be content to have a high propellant consumption, low exit temperature nuclear rocket.

No conclusions can be drawn in this investigation concerning the mechanism of triggering an excursion in an actual reactor. In order for the excursions to occur at constant pressure drop in the present apparatus the excursion had to be "forced" to proceed from the unstable laminar equilibrium point to the stable turbulent equilibrium point by shutting off the electrical heating and constantly adjusting the pressure drop to remain constant. Conversely, in a nuclear rocket the pressure drop between the plenums would always remain constant while a single errant passage might experience a flow excursion due to some disturbance.

REFERENCES

1. Longmire, Conrad: Stability of Viscous Flow Heat Exchanger, Unpublished work done at Los Alamos Scientific Laboratory July 11, 1955.
2. Bussard, R. W.; and DeLaer, R. D.: Fundamentals of Nuclear Flight. McGraw-Hill Book Company, 1965.
3. Harry, David P., III: A Steady-State Analysis of the "Laminar-Instability" Problem Due to Heating Para-Hydrogen in Long, Slender Tubes. NASA TN D-2084, 1964.
4. Gruber, A.R.; and Hyman, S. C.: Flow Distribution Among Parallel Heated Channels, Am. Inst. Chem. Eng. J. 2, 1965.
5. Reshotko, E.: An Analysis of the "Laminar Instability" Problem in Gas-Cooled Nuclear Reactor Passages. AIAA Journal, Vol. 5, No. 9, September, 1967.
6. Guevara, F. A.; McInteer, B. B.; Potter, R. M.: Temperature-Flow Stability Experiments. Los Alamos Scientific Laboratory, LAMS-2934, 1963.
7. Bankston, Charles A.: Fluid Friction, Heat Transfer, Turbulence, and Interchannel Flow Stability in the Transition from Turbulent to Laminar Flow in Tubes. Sc. D., The University of New Mexico, 1965.
8. Turney, George E.; Smith, John M.; and Juhasz, Albert J.: Steady-State Investigation of Laminar-Flow Instability Problem Resulting from Relatively Large Increases in Temperature of Normal Hydrogen Gas Flowing in Small Diameter Heated Tube. NASA TN D-3347, 1966.
9. Kolbe, E. R.: Apparatus for the Investigation of Instabilities in Gas-Cooled Heat Exchanger Tubes. Case Institute of Technology, Fluid Thermal and Aerospace Sciences TR-66-13, November, 1966.
10. Vingerhoet, P.; Reshotko, E.: Flow Excursions in a Simulated Gas-Cooled Reactor Passage. Case Western Reserve University, Fluid Thermal and Aerospace Sciences TR-68-34, September 1968.
11. Technical Catalog NCR-58, Driver-Harris Company, Harrison, New Jersey.
12. Simmons, J. T.: The Physical and Thermodynamic Properties of Helium. William R. Whittaker Company Limited Technical Report D-9027, 1957.

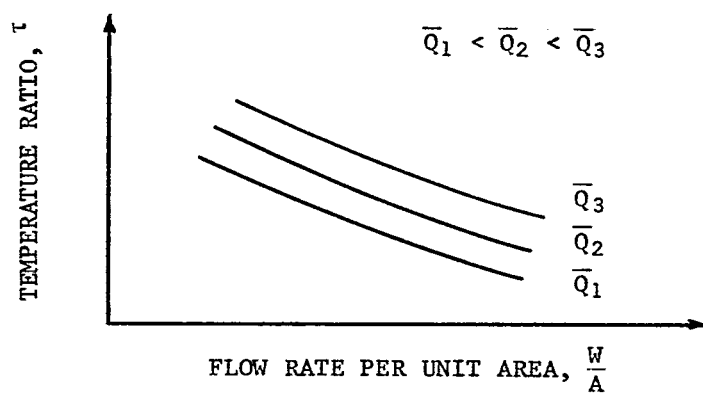
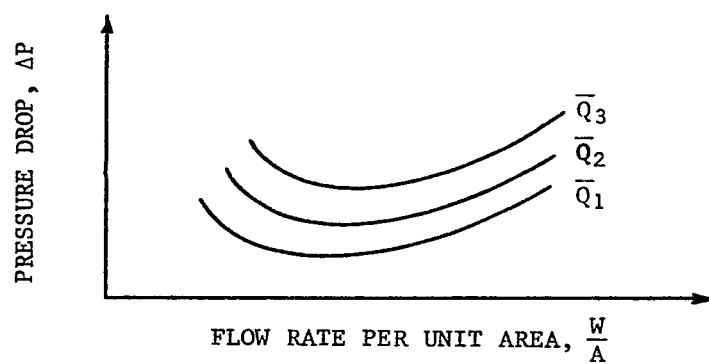


Figure 1. Representative Steady-State Characteristics

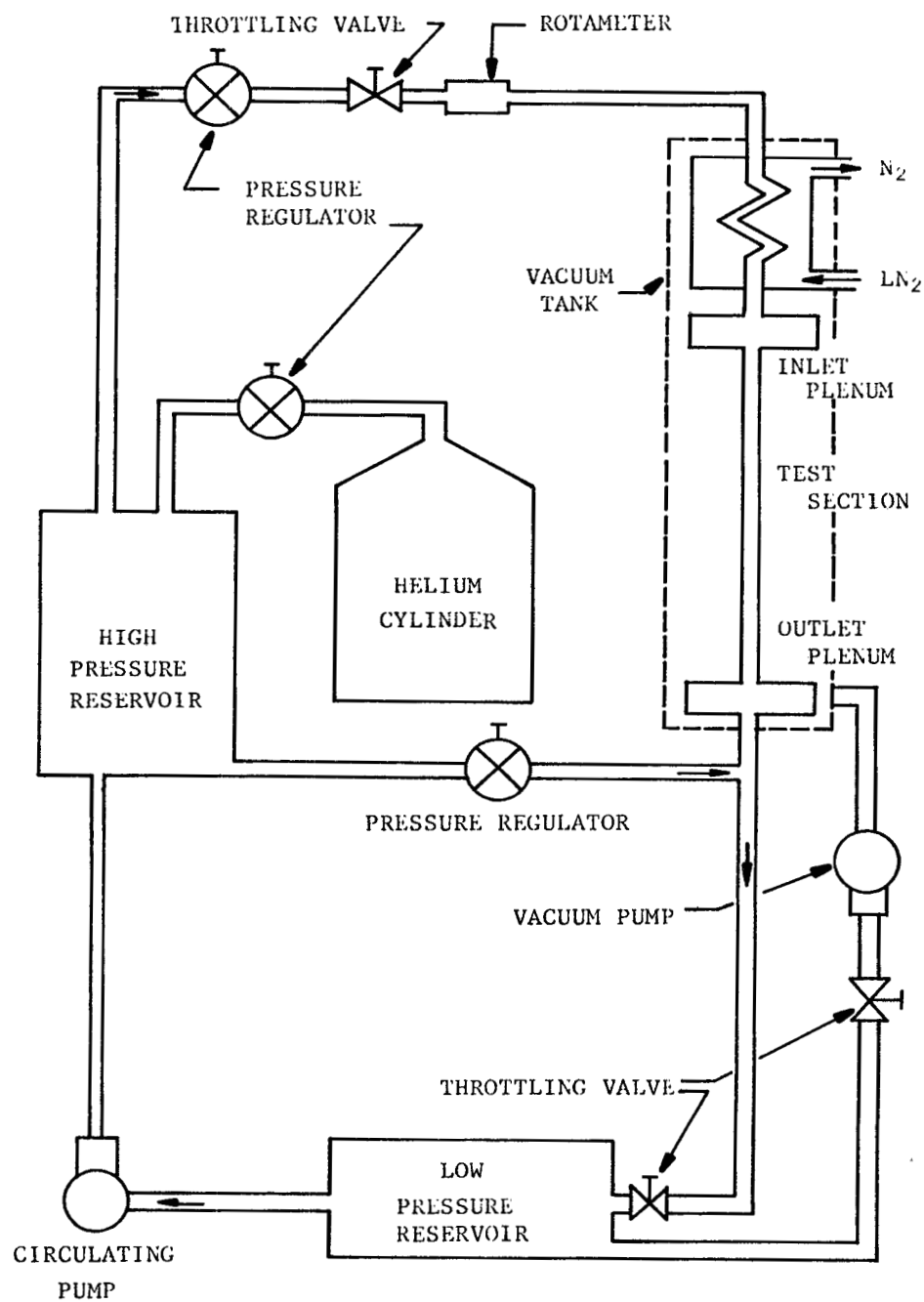


Figure 2. Flow Diagram for Experimental Apparatus

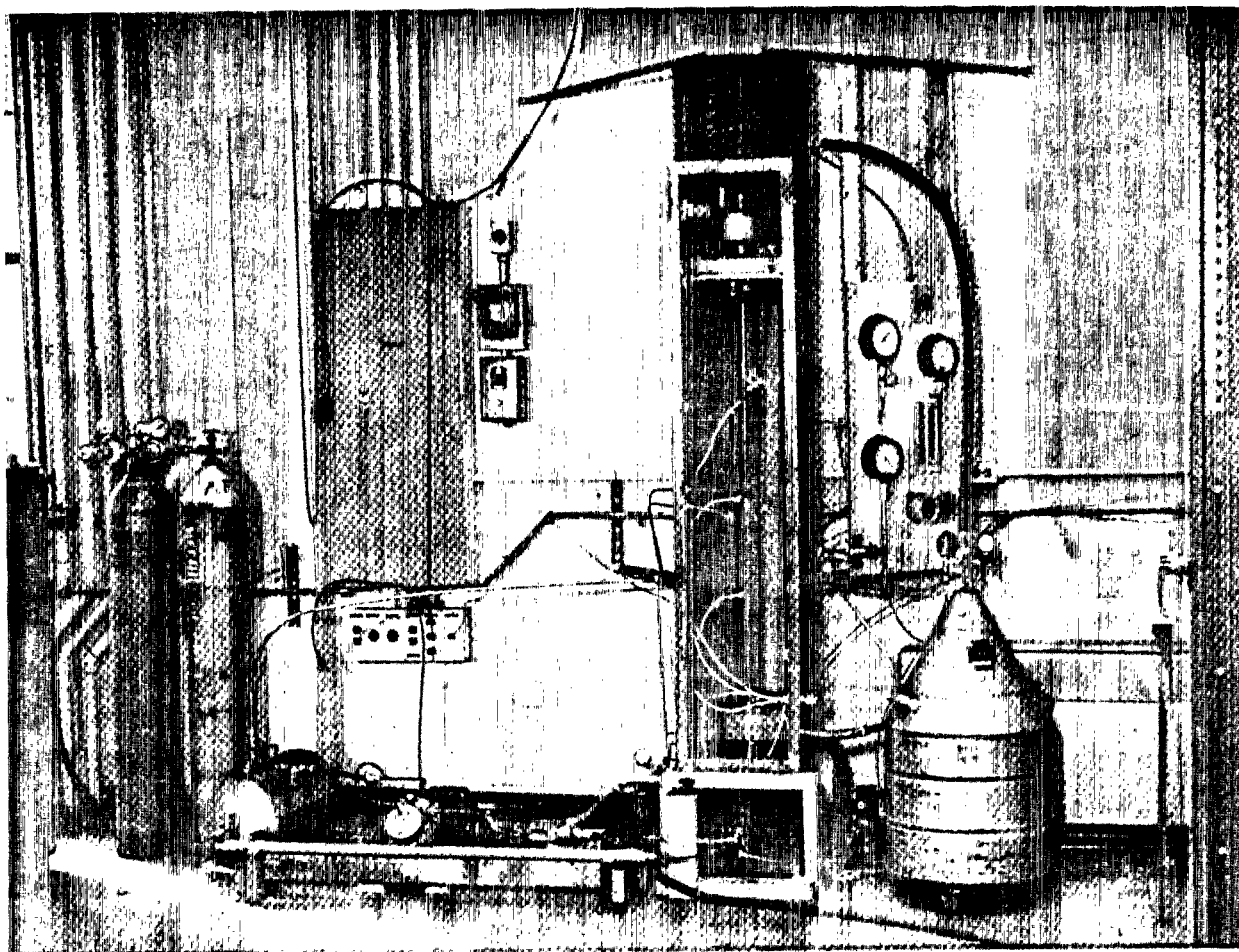


Figure 3. Instrumentation and Test Section

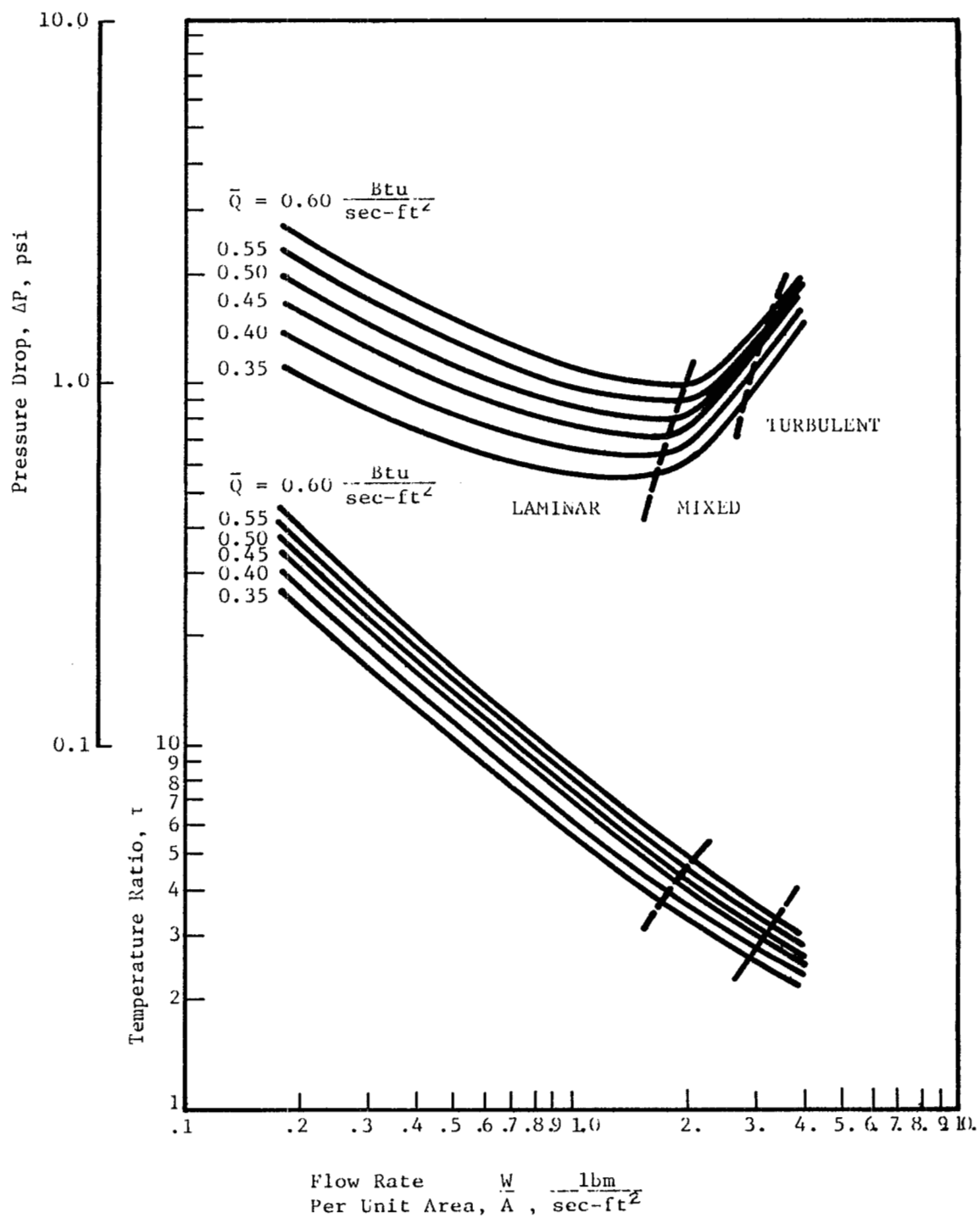


Figure 4. Theoretically Calculated Steady-State Characteristics, Helium; Inlet Pressure, 1 Psig; Inlet Temperature, 140° R; Tube Diameter, 0.094 In.; Tube Length, 4.5 Ft.

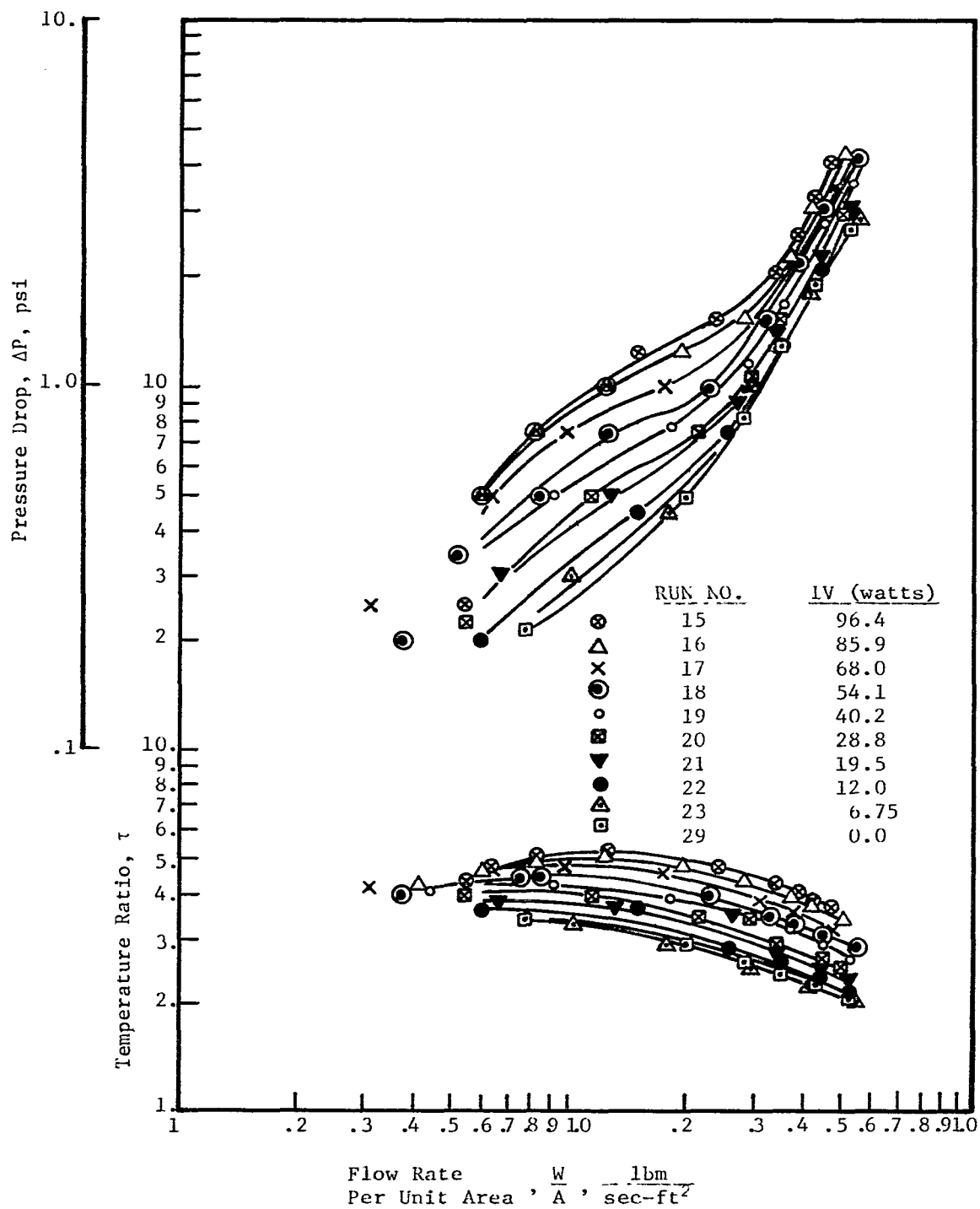


Figure 5. Experimentally Observed Steady-State Characteristics
For Constant Electrical heating
helium; Inlet Pressure, 1 Psig; Inlet Temperature, 140°R
Tube Diameter, 0.094 In.; Tube Length, 4.5 Ft.

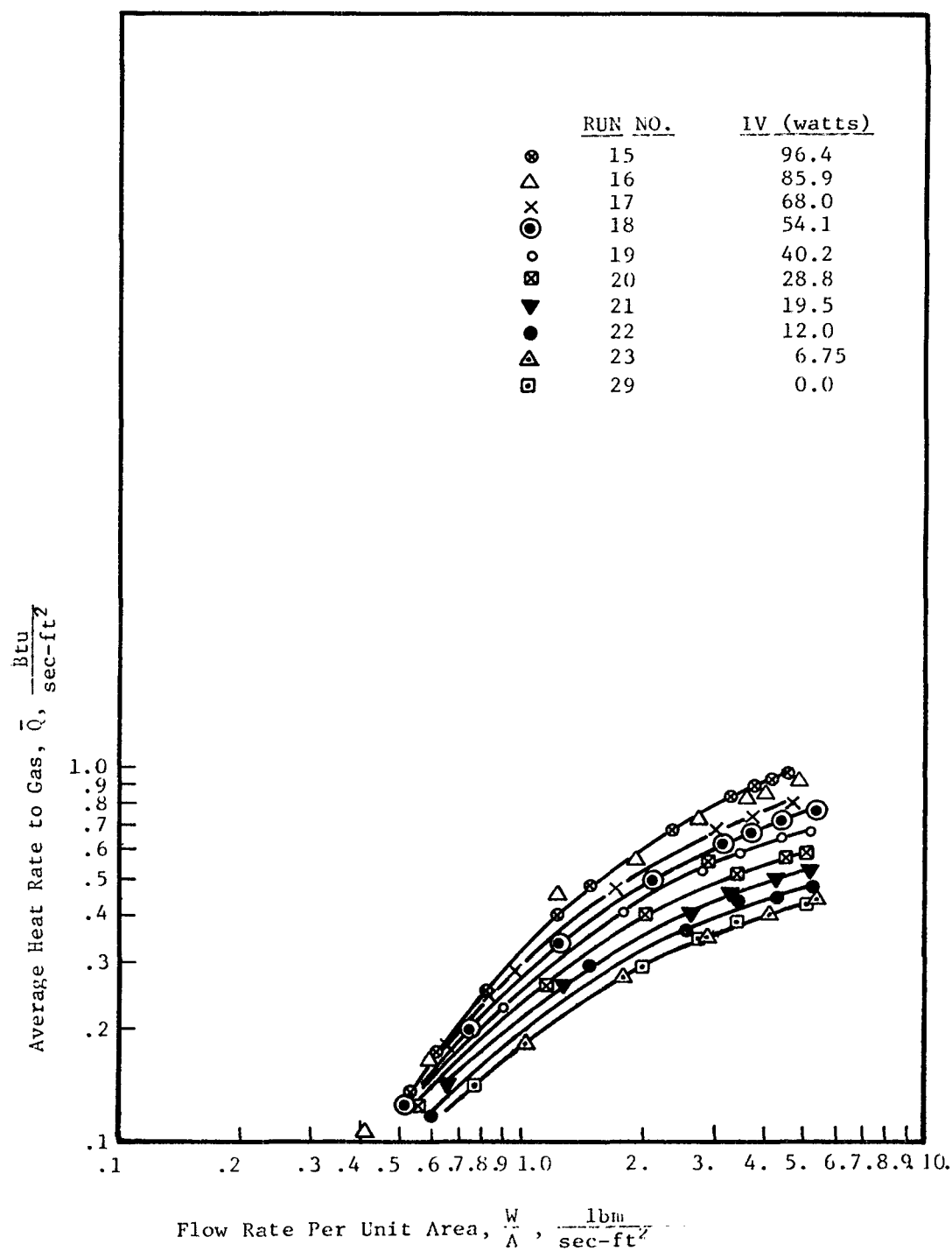


Figure 6. Calculated Heat Rate to the Gas
for Constant Electrical Heating

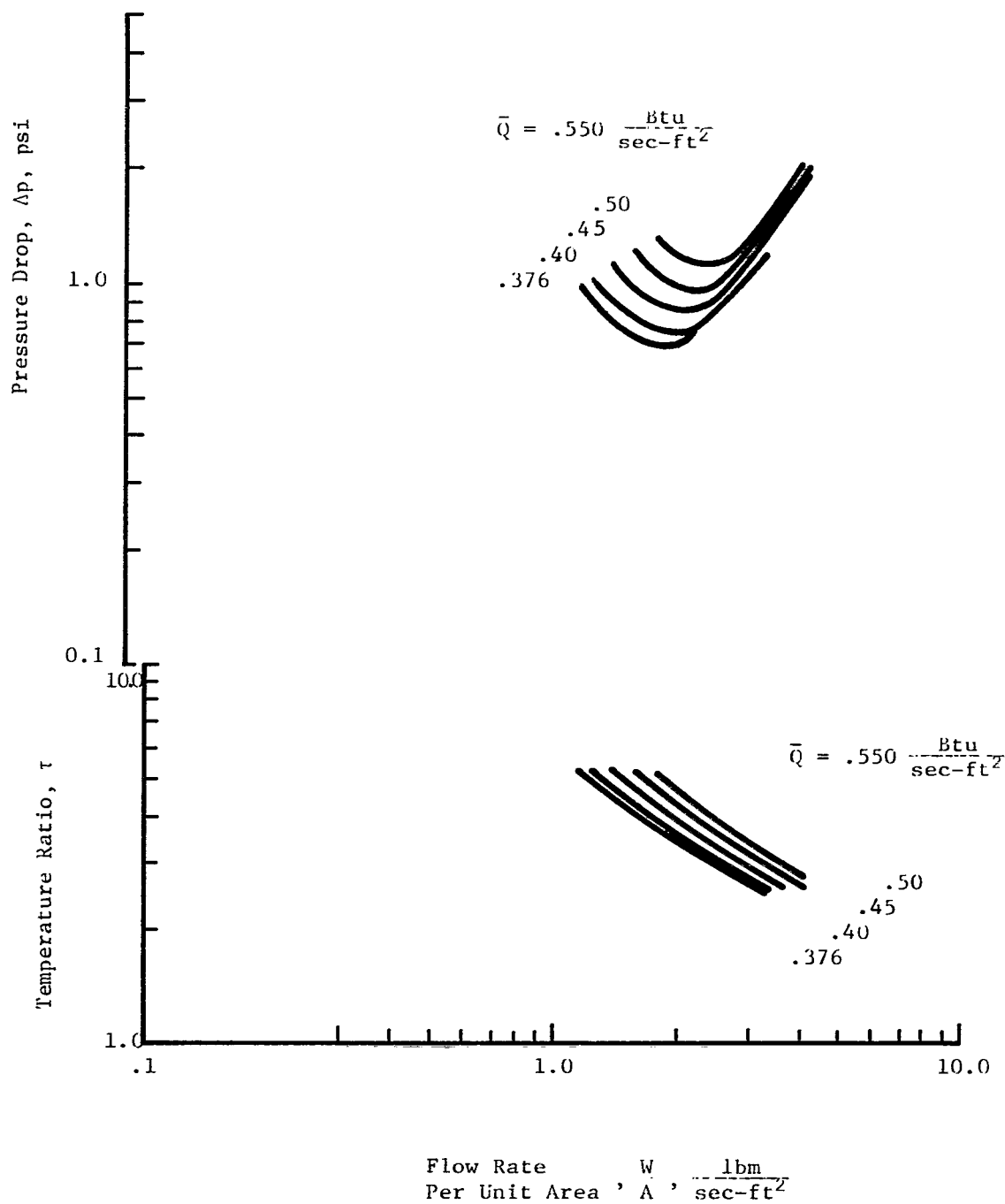


Figure 7. Experimental Steady-State Characteristics for
 Constant Heat Rate to the Gas
 Helium; Inlet Pressure, 1 psig; Inlet Temperature, 140°R
 Tube Diameter, 0.094 In.; Tube Length, 4.5 Ft.

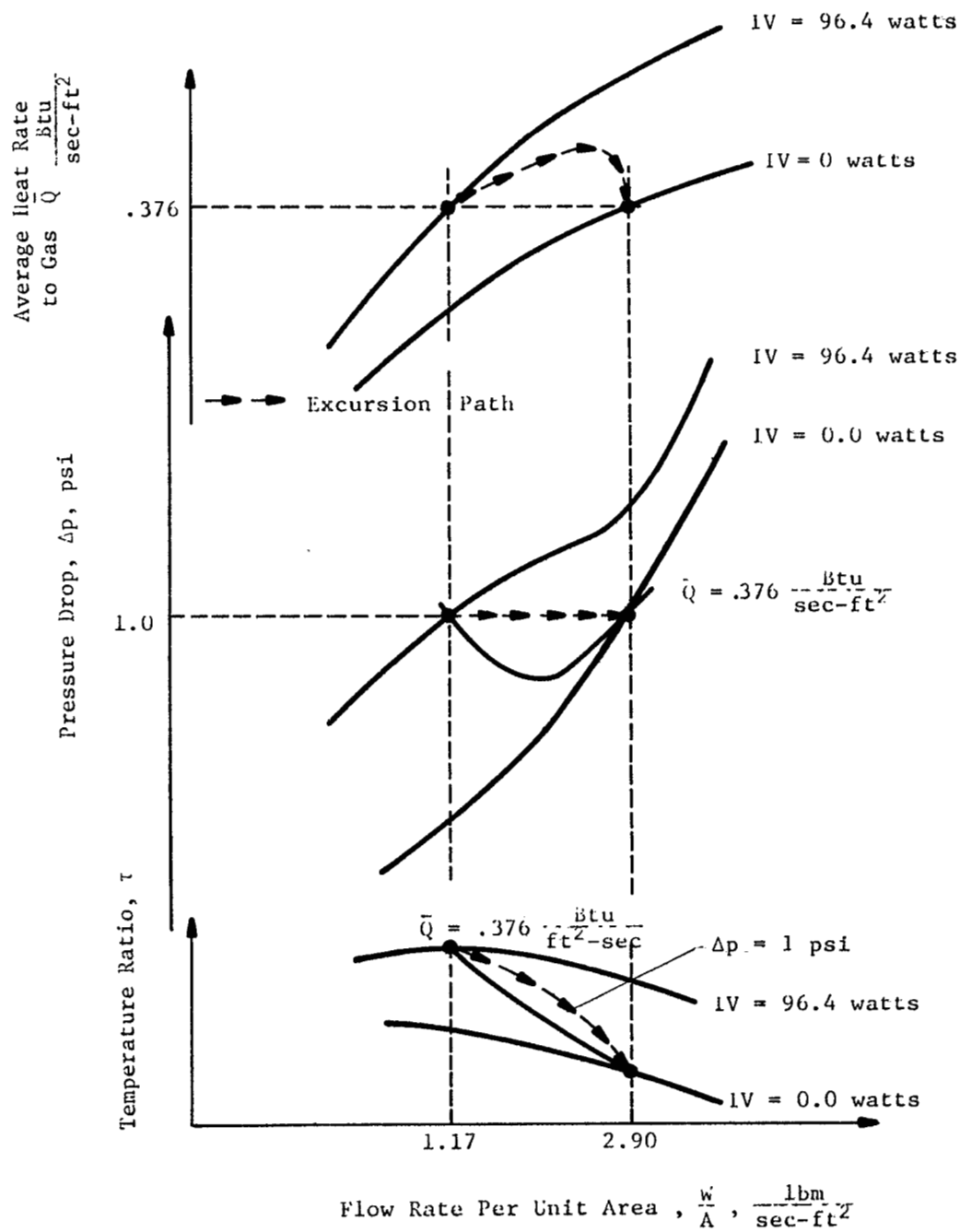


Figure 8. Schematic of Excursion Path

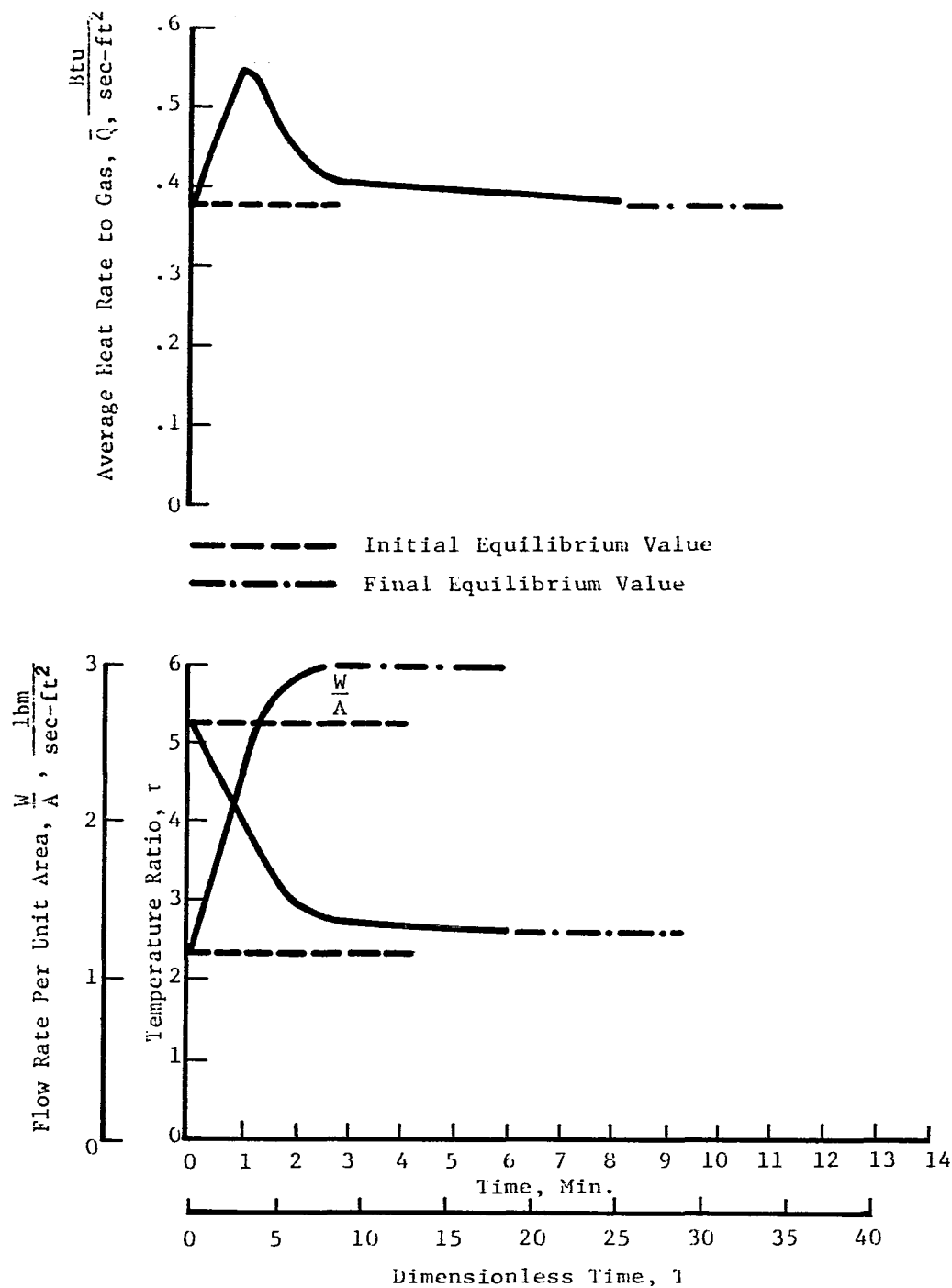


Figure 9. Experimentally Observed Excursion Characteristics

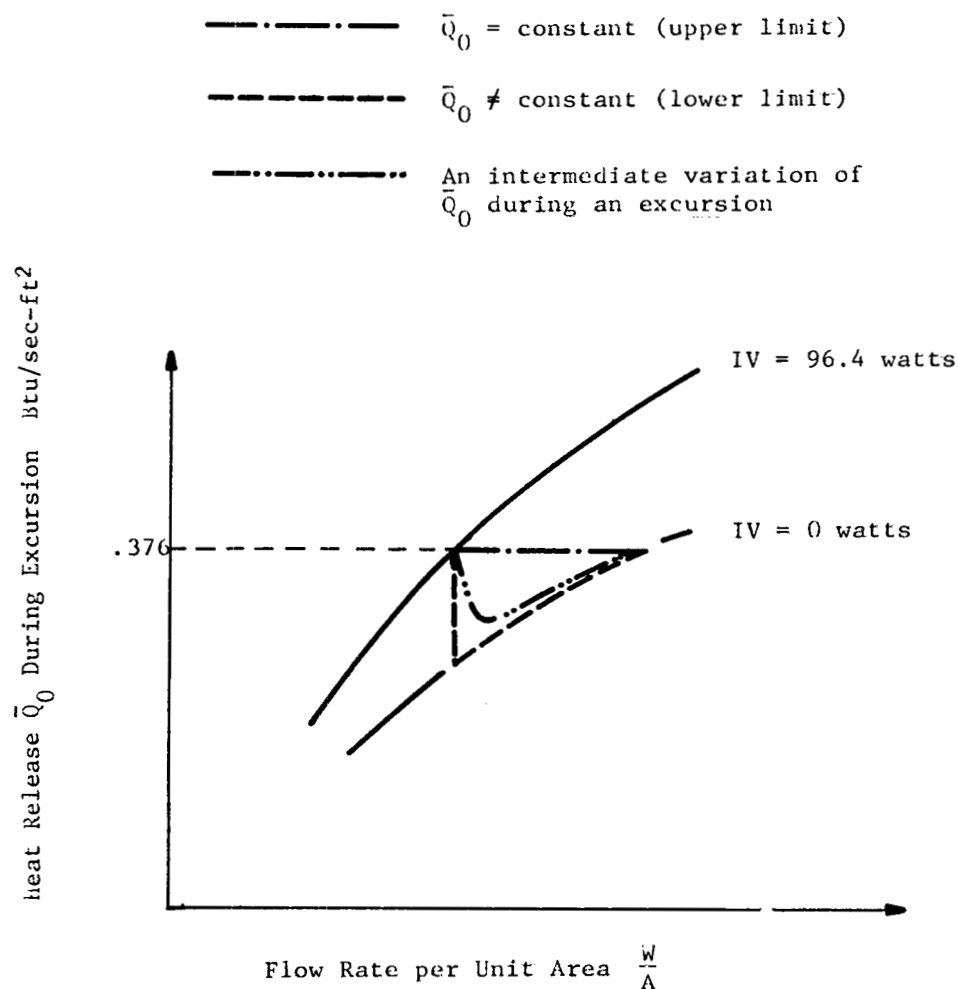


Figure 10. Possible Variation of \bar{Q}_0 During Excursion Experiment

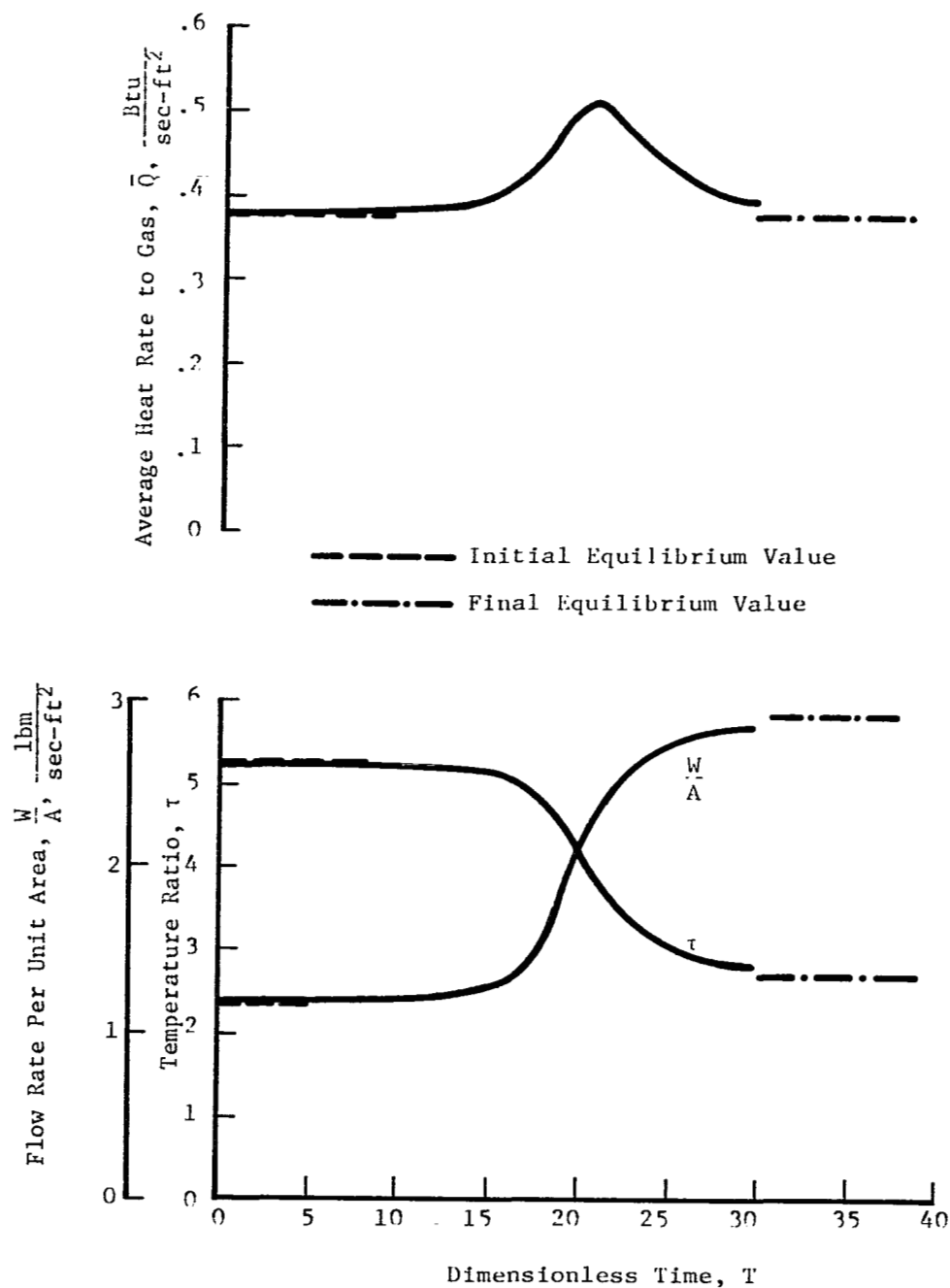


Figure 11. Excursion Characteristics Calculated From Experimentally Observed Steady-State Characteristics ($\bar{Q}_0 = \text{constant}$)

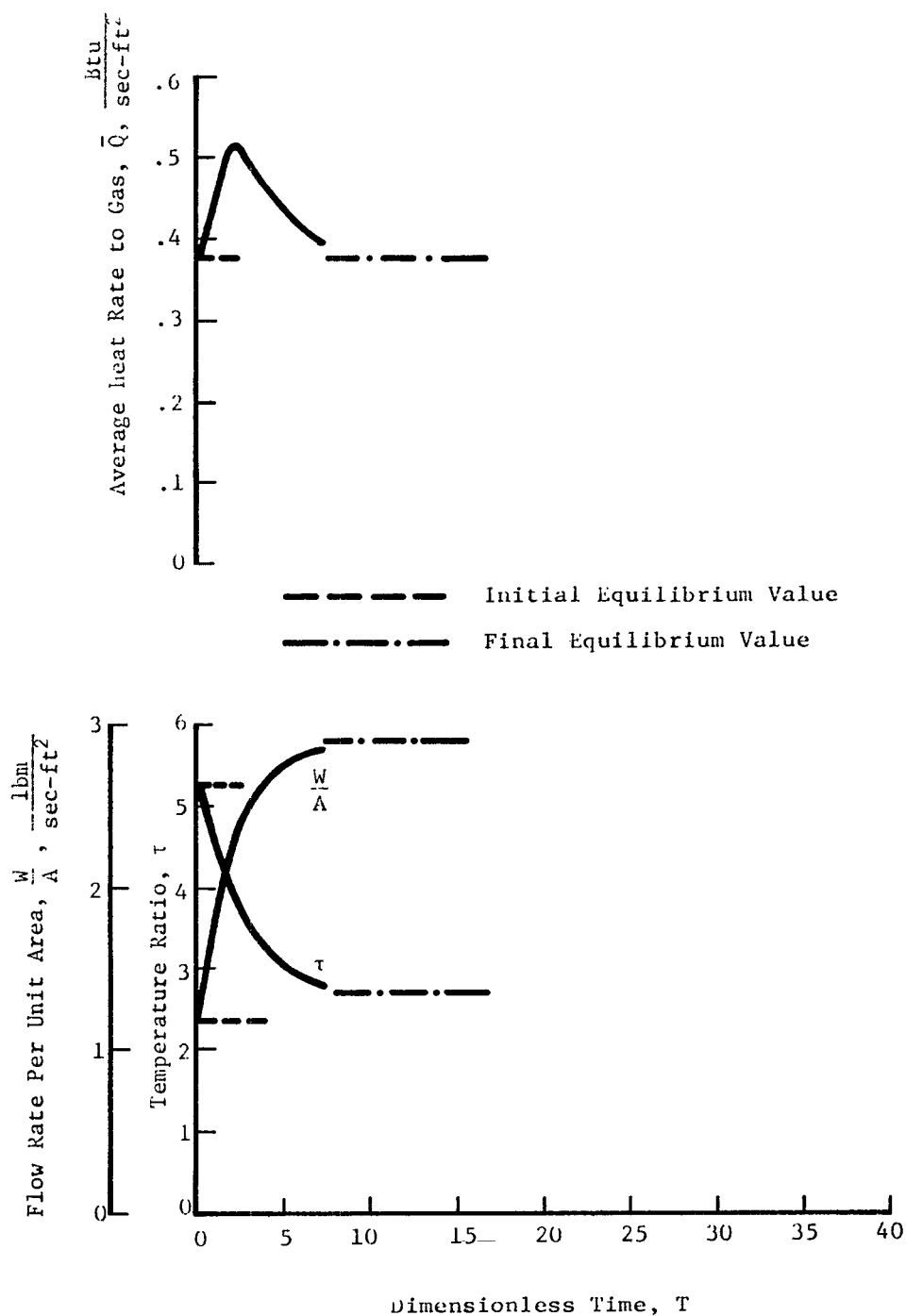


Figure 12. Excursion Characteristics Calculated From Experimentally Observed Steady-State Characteristics ($\bar{Q}_0 \neq \text{constant}$)